PHYSICS

Extremely brilliant GeV γ-rays from a two-stage laser-plasma accelerator

Xing-Long Zhu[1,2,3], Min Chen[1,3]*, Su-Ming Weng[1,3], Tong-Pu Yu[4], Wei-Min Wang[5,6], Feng He[1,3], Zheng-Ming Sheng[1,2,3,7,8]*, Paul McKenna[2,7], Dino A. Jaroszynski[2,7], Jie Zhang[1,3,6]

Copyright © 2020 The Authors, some rights reserved; exclusive licensee American Association for the Advancement of Science. No claim to original U.S. Government Works. Distributed under a Creative Commons Attribution License 4.0 (CC BY).

Recent developments in laser-wakefield accelerators have led to compact ultrashort X/γ-ray sources that can deliver peak brilliance comparable with conventional synchrotron sources. Such sources normally have low efficiencies and are limited to 10^{7-8} photons/shot in the keV to MeV range. We present a novel scheme to efficiently produce collimated ultrabright γ-ray beams with photon energies tunable up to GeV by focusing a multi-petawatt laser pulse into a two-stage wakefield accelerator. This high-intensity laser enables efficient generation of a multi-GeV electron beam with a high density and tens-nC charge in the first stage. Subsequently, both the laser and electron beams enter into a higher-density plasma region in the second stage. Numerical simulations demonstrate that more than 10^{12} γ-ray photons/shot are produced with energy conversion efficiency above 10% for photons above 1 MeV, and the peak brilliance is above 10^{26} photons s^{-1} mm^{-2} $mrad^{-2}$ per 0.1% bandwidth at 1 MeV. This offers new opportunities for both fundamental and applied research.

INTRODUCTION

Bright sources of high-energy γ-rays are versatile tools (*1*–*3*) that are applied in broad areas ranging from fundamental research (*4*–*7*) in astrophysics, particle and nuclear physics, to high-resolution imaging (*8*, *9*) in chemistry, biology, medicine, materials science, and industry. These applications can benefit greatly from the availability of further compact γ-ray sources with low divergence, short pulse duration, high energy, and high peak brilliance. At present, widely used synchrotrons (*2*) and X-ray free-electron lasers (XFELs) (*10*) can deliver X-ray pulses with peak brilliance in the range of 10^{19-24} and 10^{27-32} photons s^{-1} mm^{-2} $mrad^{-2}$ per 0.1% bandwidth (BW), respectively. However, they are normally limited to photon energies ranging from a few keV to hundreds of keV, and peak powers in the multi-GW level. In addition, the size and cost of these large research infrastructures limit access to the sources.

On the other hand, compact laser-wakefield accelerators (LWFAs) (*11*–*16*) have been developed rapidly over the past two decades (*17*) and offer a radically different approach—the acceleration length in plasmas is about three orders of magnitude smaller as compared to conventional accelerators, providing the ability to drive the acceleration and radiation of high-energy particles on a much smaller scale. Multi-GeV electron beams have been produced using LWFA (*18*), and femtosecond-scale X/γ-ray pulses in the range of keV to MeV can be produced via LWFA-based betatron radiation (*19*–*22*) and Compton backscattering (*23*–*25*). The resulting radiation sources have typical peak brilliance of 10^{19-23} photons s^{-1} mm^{-2} $mrad^{-2}$ per 0.1% BW, while the photon number per shot is limited to 10^{7-8} photons with the laser-to-photon energy conversion efficiency at a very low level on the order of 10^{-6}. Although substantial efforts have been dedicated to enhancing betatron radiation, such as using energetic particle beam–driven plasma wakefields (*26*, *27*) and increasing transverse oscillation amplitudes (*28*), it remains a great challenge to significantly increase the energy conversion efficiency and to generate collimated γ-rays with high peak brilliance on the order of the XFEL level and with high energies in the MeV to GeV regime. Currently, many cutting-edge applications and scientific research (*29*–*31*) require γ-rays with ultrahigh brilliance and photon energies far exceeding 1 MeV. These applications include exploring elementary particles (*4*), probing nuclear structures and photonuclear physics (*5*, *6*), and examining quantum processes (*7*), which rely heavily on γ-ray sources in the MeV to GeV range.

Continuous development in ultrahigh-power laser technology (*32*) provides possibilities for producing brilliant high-energy γ-ray sources. So far, considerable theory and simulation efforts have been made to develop such photon sources, based on emission of energetic electrons accelerated in extreme laser fields, such as laser interactions with near-critical-density plasmas (*33*–*35*), laser-driven radiation reactions (*36*–*38*), laser-irradiated solid interactions (*39*–*41*), laser scattering off electrons (*42*, *43*), and the excitation of electromagnetic cascades (*44*, *45*). However, there are unavoidable physical limitations on the γ-ray peak brilliance with these methods, such as a very large divergence in direct laser interaction with electrons. Furthermore, an exceptionally high laser intensity of 10^{23-25} W/cm^2 (two to four orders of magnitude higher than the highest intensities available to date) is required to produce GeV photons. This requires tens-of-petawatt (PW) laser pulses to be focused to near-diffraction-limited spots, which is very challenging. As soon as the laser intensity is reduced to the order of ~10^{21} W/cm^2 (which is the highest intensity level of reliable operation of current high-power laser systems), the methods mentioned above become intrinsically inefficient for γ-ray emission. In addition, the ability to tune the photon energy, power, and brilliance is limited. It has been recently proposed that collimated γ-rays may be produced when ultradense relativistic electrons interact with conductors via beam-plasma instabilities (*46*),

[1]Key Laboratory for Laser Plasmas (MOE), School of Physics and Astronomy, Shanghai Jiao Tong University, Shanghai 200240, China. [2]SUPA, Department of Physics, University of Strathclyde, Glasgow G4 0NG, UK. [3]Collaborative Innovation Center for IFSA, Shanghai Jiao Tong University, Shanghai 200240, China. [4]Department of Physics, National University of Defense Technology, Changsha 410073, China. [5]Department of Physics, Renmin University of China, Beijing 100872, China. [6]Institute of Physics, Chinese Academy of Sciences, Beijing 100190, China. [7]Cockcroft Institute, Sci-Tech Daresbury, Cheshire WA4 4AD, UK. [8]Tsung-Dao Lee Institute, Shanghai Jiao Tong University, Shanghai 200240, China.
*Corresponding author. Email: minchen@sjtu.edu.cn (M.C.); z.sheng@strath.ac.uk (Z.-M.S.)

but the required high-density GeV electron beams are well beyond current technical capabilities. Heretofore, there is no alternative method applicable to achieve the peak brilliance of γ-ray sources comparable to the XFEL level.

Here, we introduce a new efficient scheme to produce extremely high-brilliance γ-rays with photon energies up to GeV, which is based on a two-stage LWFA driven by a single multi-PW laser pulse. The first stage, using a moderately low-density plasma, produces a multi-GeV electron beam with a high energy efficiency of ~40%, while the second stage using a relatively high-density plasma produces MeV-GeV γ-ray radiation with an efficiency over 10%. The resulting photon number, energy efficiency, peak brilliance, and power are several orders of magnitude higher than existing LWFA-based sources. This may pave the way for applications in broad areas of science and technology that require high-brilliance γ-rays with photon energy in the MeV to GeV regime.

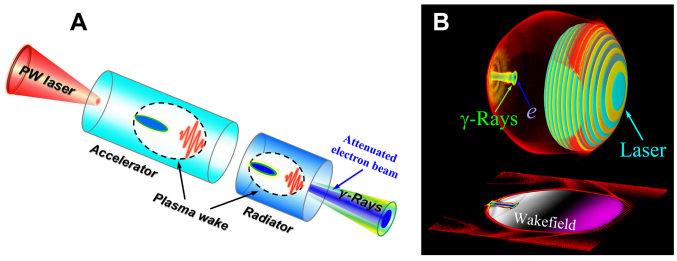

Fig. 1. Concept of the compact bright γ-ray source. (**A**) Schematic of the two-stage scheme. In the first acceleration stage, a plasma wake is driven by a multi-PW laser pulse propagating in an underdense plasma channel, where efficient electron injection and acceleration result in a multi-GeV, low-emittance, high-charge, and high-density electron beam. The laser pulse then enters a higher-density plasma region that acts as a radiator, where collimated bright γ-rays are produced by the dense high-energy electrons in the enhanced electrostatic fields of the bubble in the denser plasma. (**B**) Three-dimensional (3D) view of the γ-ray radiation in laser-driven plasma wakefield using a 3D particle-in-cell (PIC) simulation. Simulation parameters are mentioned in Methods.

RESULTS

Physical scheme

It is well known that a low-density plasma is beneficial for accelerating trapped electrons to high energies because the electron dephasing length (*17*) $L_{\mathrm{deph}} \propto 1/n_e$, where n_e is the plasma density. However, strong betatron oscillations preferentially occur in a high-density plasma, which enhances betatron radiation with a critical photon energy $\hbar\omega_{\mathrm{crit}} \propto \left(\frac{\epsilon_e}{m_e c^2}\right)^2 n_e r_\beta$, where c is the speed of light in vacuum and ϵ_e, m_e, and r_β are the electron energy, mass, and transverse oscillation amplitude, respectively. This contradiction severely restricts betatron emission in the wakefield to photon numbers in the range 10^{7-8} and photon energy in the hundreds of keV range, thus only achieving peak brilliance comparable to the synchrotron radiation.

To overcome this problem, we propose a two-stage scheme that combines the advantages of efficient electron acceleration in a moderately low-density LWFA and efficient photon emission from energetic electrons in a relatively high-density LWFA, as shown in Fig. 1. Here, a multi-PW laser pulse is focused to a currently achievable intensity of ~10^{21} W/cm^2, enabling it to drive a plasma bubble in a relatively high-density (~10^{20} cm^{-3}) plasma according to the similarity of relativistic laser-plasma interactions (*47*) $S = \frac{n_e}{a_0 n_c}$, where $a_0 = \frac{eE_y}{m_e c\omega_0}$ is the normalized laser amplitude, e is the unit charge, $\omega_0 = \frac{2\pi c}{\lambda_0}$ is the laser frequency, and $n_c = \frac{m_e\omega_0^2}{4\pi e^2}$ is the critical plasma density. In addition, a plasma channel with a transverse parabolic density profile is used to guide the high-power laser (*17*, *18*).

In the first stage, the plasma electrons are self-injected and accelerated in the plasma bubble excited by the multi-PW laser pulse propagating in an underdense plasma, resulting in a low-divergence, tens-nC, and multi-GeV electron beam with a high beam density close to the critical plasma density (10^{21} cm^{-3}). The laser-to-electron energy conversion efficiency is up to ~40%. It should be pointed out that if we only consider the accelerated electrons around the quasi-monoenergetic peak, the efficiency is about 22%, consistent with the result (~20%) predicted by Gordienko and Pukhov (*47*). In the second stage, the laser pulse propagates into the relatively high-density plasma, resulting in a shrunken plasma bubble as the density increases. Besides the accelerated GeV electrons from the previous stage, additional electrons are injected in this stage, which further increases the total charge of the accelerated electron beam with a peak density well above the critical density. The efficiency increases to above 50% for the total accelerated GeV electrons as well. This results in large quasi-static electromagnetic fields around the electron beam with a radiation parameter as high as $\chi_e \sim 0.1$ defined in the following, as we can see later, which gives rise to emission of a collimated beam of γ-rays with photon energies up to the GeV level. Because the quasi-static electromagnetic fields are high enough, the radiation reaction and quantum effects begin to play an important role in the photon emission process (*33*, *37*). A distinct feature of this scheme is the high efficiency of both electron acceleration and radiation. The efficiency of multi-GeV tens-nC electrons produced is as high as 50% with an energy gain above 100 J, giving rise to an unprecedented radiation efficiency for γ-rays (with photon energy above 1 MeV) in excess of 10%, as will be shown later. Consequently, the photon number, efficiency, peak brilliance, and power of the γ-rays emitted are several orders of magnitude higher than current LWFA betatron radiation (*19*–*22*) and Compton (*23*–*25*) sources.

Extremely bright γ-ray emission

To obtain collimated ultrabright high-energy γ-ray pulses, both the charge and energy of the accelerated electron beam and the quasi-static electromagnetic fields should be high enough. To fulfill these conditions, the plasma density is longitudinally tailored to form two successive stages, one with moderately low density for efficient acceleration and the other with relatively high density for efficient radiation (see Fig. 2A).

In the acceleration stage, a plasma wake with an ultrahigh acceleration gradient above 20 GV/cm is produced by the drive laser pulse in a moderately low-density plasma channel (see Fig. 2, B and C) so that a large number of electrons are rapidly accelerated by the wake to GeV energy in millimeters. The laser pulse, together with its accelerated electron beam, then enters a higher-density plasma region in the radiator stage, where both the accelerating field ($E_x \propto \sqrt{n_e}$) and the laser fields (through relativistic self-focusing) are enhanced significantly, even though the laser depletion and electron dephasing occur faster, as shown in Fig. 2, D and E. This results in a high-density

(10^{21} cm^{-3}), high-charge (tens-nC), and multi-GeV electron beam (Fig. 2F). Because of high-efficiency electron acceleration occurring in high-power ultra-intense laser-plasma interactions, collimated γ-rays with photon energies up to the GeV level are copiously emitted within a narrow angular range (Fig. 2, G and H). We consider the γ-rays emitted in a 0.1% energy BW within an angle of 5 mrad, with a source size of 2 μm and a duration of 30 fs at full width at half maximum (FWHM), which gives a peak brilliance about 4×10^{26} photons s^{-1} mm^{-2} mrad^{-2} per 0.1% BW at 1 MeV and 1.2×10^{26} (usual units) at 20 MeV, as shown in Fig. 2I. One can see that the maximum peak brilliance of γ-rays may reach up to the XFEL level, making them promising high-brilliance high-energy radiation source for fundamental research and practical application.

To illustrate the physical processes occurring in the two stages, we show the evolution of the plasma wake, transverse field, and radiation parameter in Fig. 3. In the acceleration stage, injection and stable acceleration of electrons are observed. The charge of trapped electrons with energy above 1 GeV is as high as 35 nC. They are accelerated to a maximum energy of ~3.6 GeV at ct = 1500 μm. When the laser pulse propagates into the radiator stage with a higher plasma density, the bubble shrinks as $\lambda_w \approx 2\pi c\sqrt{a_0}/\omega_p$, where $\omega_p = \sqrt{4\pi n_e e^2/m_e}$ is the plasma frequency. The acceleration field ($E_x \propto \sqrt{n_e}$) is simultaneously increased and has a decreased phase velocity (*17*). As a result, more electrons can be trapped and accelerated (with a charge up to ~40 nC above 1 GeV). This further enhances the self-generated fields because they scale as $2\pi e n_b r_b^2/r$, for $r > r_b$ and $2\pi e n_b r$ for $r \le r_b$, where n_b and r_b are the electron beam density and radius. The quasi-static transverse electromagnetic fields ($F_\perp$) are composed of two parts: one component induced by the accelerated electron beam and the other associated with the plasma electron cavity (scaling as $m_e\omega_p^2 r/2e$). As expected, with the increase of both n_e and n_b, $F_\perp$ is greatly enhanced (Fig. 3D). This leads to a large radiation parameter χ_e (Fig. 3F), which is proportional to ϵ_e and $F_\perp$ as $\chi_e \approx \left(\frac{e\hbar}{m_e^3c^5}\right)\epsilon_e F_\perp$ (see Methods). Our simulations

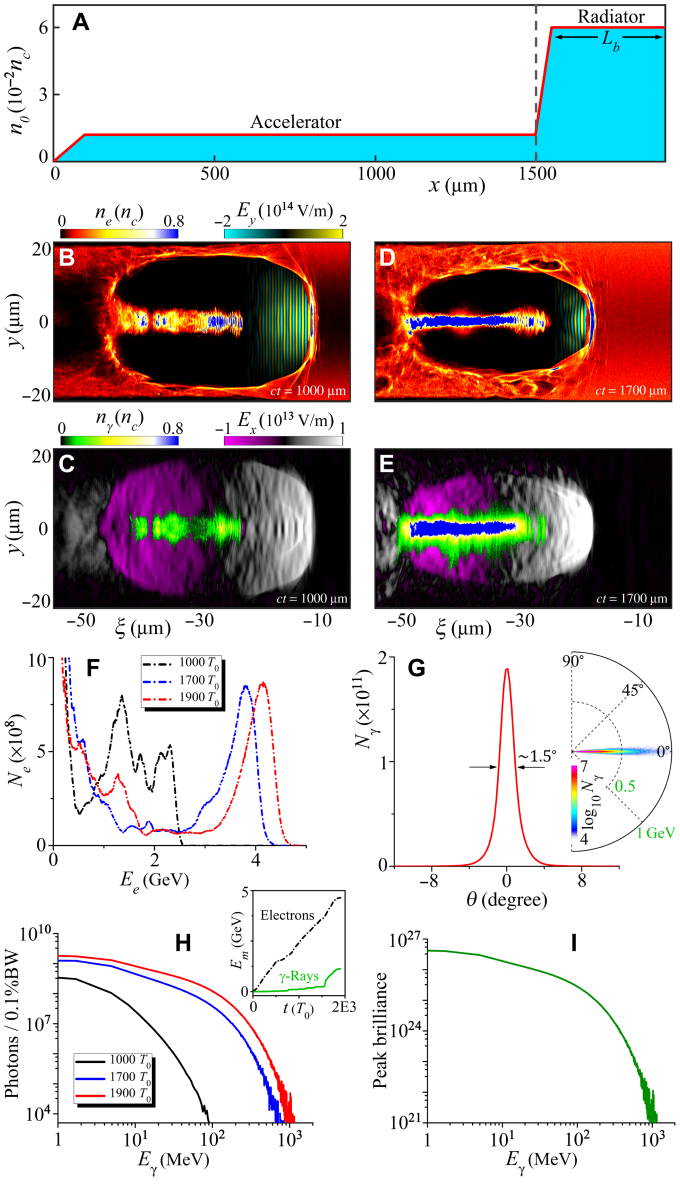

Fig. 2. The laser-plasma accelerator-radiator setup and 3D PIC simulation results. (**A**) On-axis density profile of the background plasma. (**B** and **D**) Snapshots of distributions of the electron density (n_e) and laser field (E_y) are shown at time ct = 1000 μm and ct = 1700 μm, respectively, in the acceleration and radiation stages, where ξ = x − ct. Corresponding snapshots of distributions of the photon density (n_γ) and accelerating field (E_x) are presented in (**C**) and (**E**), respectively. The energy spectra of electrons (**F**) and γ-rays (**H**) at given times. In (H), the inset shows the temporal evolution of the maximum energy of electrons and γ-rays. (**G**) Angular spectrum and angular distribution of γ-rays. (**I**) γ-Ray peak brilliance (photons s^{-1} mm^{-2} mrad^{-2} per 0.1% BW) as a function of the emitted photon energy.

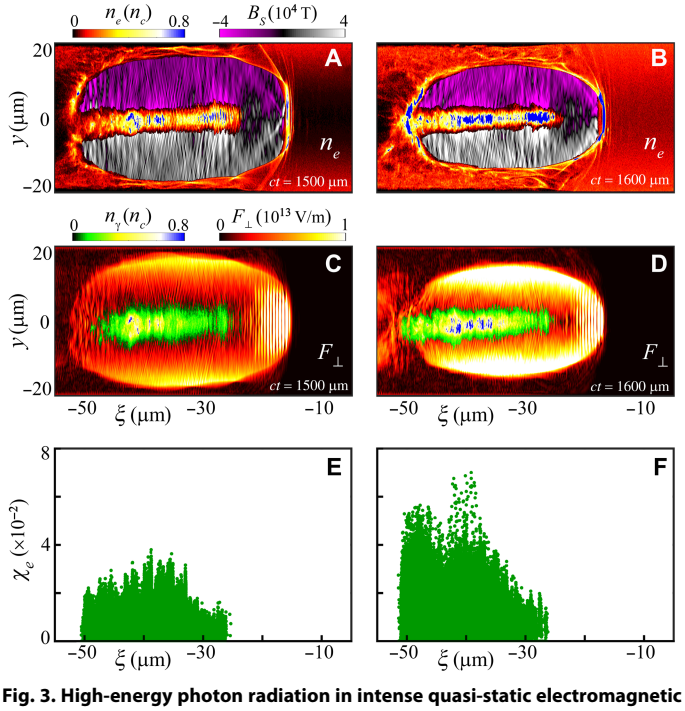

Fig. 3. High-energy photon radiation in intense quasi-static electromagnetic fields. (**A** and **B**) Distributions of the electron density (n_e) and self-generated magnetic field (B_S) at ct = 1500 μm and ct = 1600 μm, respectively. (**C** and **D**) Corresponding γ-ray photon density (n_γ) and transverse electromagnetic field ($F_\perp$). (**E** and **F**) Corresponding radiation parameter (χ_e) at the two positions mentioned above.

suggest that the radiation parameter can be as high as χ_e~0.1 (see fig. S6), which is much larger than that in typical laser-irradiated solids (*39*) ($\chi_e \lesssim 0.05$, producing multi-MeV photons with a very large divergence FWHM of >20°), although our laser intensity is even an order of magnitude lower. Consequently, the emission of radiation by energetic electrons in a wakefield enters into the high field (strong radiation reaction) regime, in which both radiation reaction and quantum effects come into play (*48*, *49*) and copious γ-ray photons are emitted in the radiator stage.

The maximum energy, peak brilliance, and radiation power of the emitted γ-ray can be tuned simply by changing the plasma parameters. Here, we mainly consider the effect of tuning the radiator on the γ-ray emission. The acceleration stage accelerates self-injected electrons to multi-GeV energies with a relatively low γ-ray emission level, compared with that in the radiation stage. We first discuss the effect of the radiator length L_b on the γ-ray emission. Figure 4A shows the results of varying L_b from 12 to 300 μm, while keeping all other parameters fixed. It shows that an appropriately long plasma radiator benefits γ-ray emission. This is due to the increased energy gain of electrons accelerated in the longer plasma segment, because $\epsilon_e \approx eE_xL$, which gives a very high efficiency (51.8%). This enables emission of copious high-energy γ-ray photons because of the substantial increase of the radiation power $P_\gamma \approx \left(\frac{2\alpha_f\hbar e^2}{3m_e^4c^6}\right)\epsilon_e^2F_\perp^2$, where the power scales approximately as $P_\gamma \propto L^2$ due to the increase in ϵ_e. However, the maximum radiator length and hence the maximum photon energy are limited, due to the laser pulse energy depletion and electron dephasing, e.g., for $L_b \gtrsim 250$ μm.

Figure 4B illustrates the effect of plasma density on the γ-ray emission, where the product of the plasma density and length is fixed as $n_0L_b = 18n_c$ μm in the radiator region, and all other parameters are unchanged. The results show that γ-ray emission enhances significantly with the increase of the plasma density because $P_\gamma \propto \epsilon_e^2F_\perp^2 \propto n_e$, where $\epsilon_e \approx eE_xL \propto 1/\sqrt{n_e}$ and $F_\perp \propto \frac{m_e\omega_p^2r}{2e} \propto n_e$. For example, using a density of $1.2n_c$, γ-ray pulses in the energy range up to 3 GeV are obtained with a peak brilliance of ~8×10^{26} photons s^{-1} mm^{-2} $mrad^{-2}$ per 0.1% BW at 1 MeV and 12.5% conversion efficiency. The corresponding peak power is up to ~1 PW. This enables a substantial amount of electron energy to be efficiently transferred to high-energy photons. It should be noted, however, that the radiator density should not be too high, as it will deplete the laser pulse energy rapidly and shorten the acceleration distance ($L_b \propto 1/n_0$). This limits the electron energy gain and thus photon emission, causing the saturation of radiation power and photon energy.

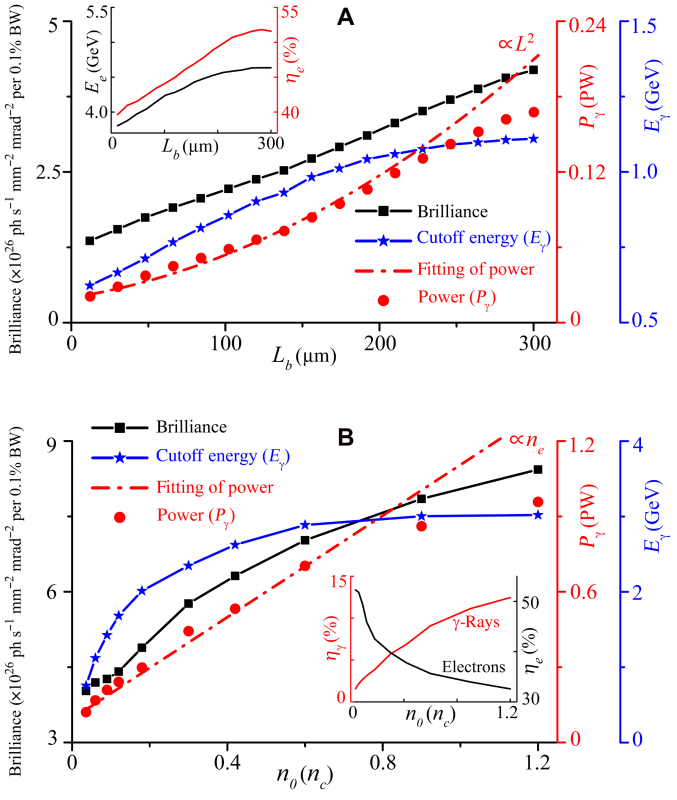

Fig. 4. Effect of the plasma parameters on the γ-ray emission. (**A**) Effect of the radiator length (L_b) on the peak brilliance at 1 MeV, cutoff energy, and radiation power of the γ-rays. The inset shows the maximum energy and total efficiency of accelerating electrons above 1 GeV. (**B**) Effect of the plasma density (n_0) in the radiator region on the γ-ray peak brilliance, cutoff energy, and radiation power. The inset shows the energy conversion efficiency of trapped electrons (≥1 GeV) and γ-rays (≥1 MeV) from the drive laser. The cutoff energy of the γ-rays is defined at 10^{-5} of the peak brilliance at 1 MeV.

DISCUSSION AND CONCLUSION

To demonstrate the robustness of this γ-ray radiation scheme, in Fig. 5, we have shown a series of simulations for laser intensities varied in the range 1.6×10^{21} to 6.5×10^{21} W/cm^2. The results show that the γ-ray emission becomes more efficient as the laser intensity increases according to $P_\gamma \approx \left(\frac{2\alpha_f\hbar e^2}{3m_e^4c^6}\right)\epsilon_e^2F_\perp^2 \propto I_0^2$, where the electron energy scales as (*47*) $\epsilon_e \propto \sqrt{P_l} \propto \sqrt{I_0}$, with $P_l = I_0\pi r_0^2/2$, and the transverse field scales as $F_\perp \propto n_e \propto \sqrt{I_0}$ following from the relation $n_e = Sa_0n_c$. Energy conversion from laser to γ-rays is defined as $\eta = \varepsilon_\gamma/\varepsilon_l \propto P_\gamma/P_l$. Thus, one can obtain $\eta \propto I_0$, which agrees well with the simulation results shown in Fig. 5. As an example, using a laser

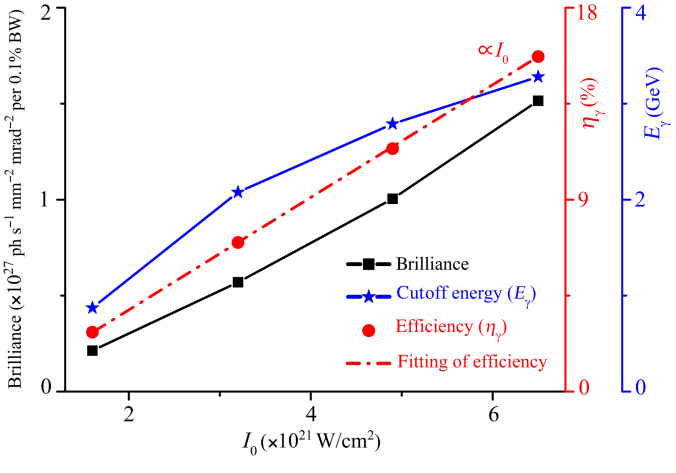

Fig. 5. Scaling of γ-ray emission with laser intensity. Effect of the laser intensity on the peak brilliance at 1 MeV, cutoff energy, and conversion efficiency of γ-ray pulses. For high-efficiency bright γ-ray emission, the radiator plasma has a density determined by a fixed parameter $S = n_0/a_0n_c = 8 \times 10^{-3}$ and length $L_b = 100$ μm. The plasma structure, all other parameters, and corresponding *S* are the same as those shown in Fig. 2.

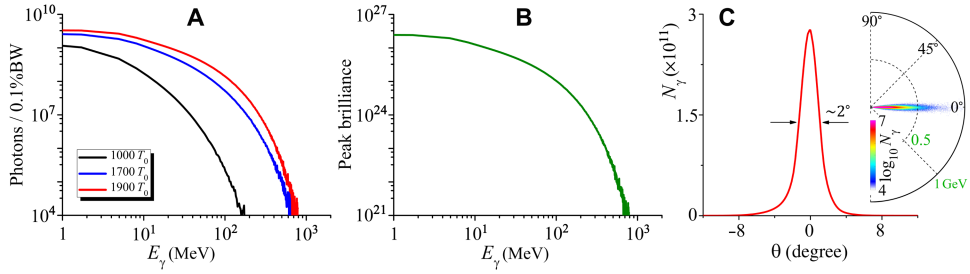

Fig. 6. Extremely bright γ-ray source generated from a two-stage self-guided laser-plasma accelerator. (**A**) Energy spectra of the γ-ray evolution with time. (**B**) Peak brilliance (photons s^{-1} mm^{-2} $mrad^{-2}$ per 0.1% BW) of the γ-rays emitted as a function of the photon energy. (**C**) Angular spectrum and angular distribution of the γ-rays.

pulse at the intensity 6.5×10^{21} W/cm^2, the γ-ray emission can reach photon energies up to 3.3 GeV, with ~16% conversion efficiency and ultrahigh peak brilliance 1.5×10^{27} photons s^{-1} mm^{-2} $mrad^{-2}$ per 0.1% BW at 1 MeV. When the laser intensity is reduced to 1.6×10^{21} W/cm^2 with a peak power of 2.5 PW, bright γ-ray radiation is still quite efficient. Therefore, this scheme has the potential to operate widely in laboratories in the near future and paves the way toward a new generation of high-efficiency ultrabright GeV γ-ray sources to a broad community.

We also discuss the performance of this radiation scheme in the self-guided LWFA case without the preformed plasma channel, as illustrated in Fig. 6. To extend this radiation scheme into the self-guided LWFA, the initial plasma parameters need to be adjusted accordingly, where the background density is set to $n_0 = 0.03n_c$ and $0.078n_c$ in the acceleration stage and the radiation stage, respectively. The laser parameters are the same as those presented in Fig. 2, and other parameters are unchanged but with doubled the simulation window size and corresponding grid cells. It is shown that the γ-ray radiation produced in the self-guided LWFA is still very brilliant with the peak brilliance on the order of the plasma channel case, even though the divergence angle becomes large and the emitted photon energy decreases considerably.

In summary, the previously reported X/γ-ray radiation sources from laser-driven plasma wakefields were limited to photon numbers of 10^{7-8} at hundred keV energies and GW powers, thus only delivering the pulse brilliance in the level of synchrotron light sources and radiation efficiency on the order of 10^{-6}. These restrict their practical applications in broad areas. Here, we propose a novel and robust scheme capable of achieving several orders of magnitude increase in the photon number, radiation efficiency, brilliance, and power of the emitted γ-rays, based on the all-optical two-stage LWFA driven by multi-PW laser pulses. This enables the development of compact ultrashort γ-ray sources with unprecedentedly high-brilliance and PW-level powers in the GeV regime. Such powerful γ-rays may offer unique capabilities and serve as a promising new platform for various applications, such as photonuclear reactions (*5*, *6*), light-light/matter interactions (*7*, *29*–*31*), and γ-ray colliders (*4*, *50*, *51*).

METHODS

γ-Ray emission

It is well-known that the accelerating electrons trapped in plasma wakefields can radiate high-energy photons via betatron oscillations (*20*–*22*). When the radiated photon energy becomes comparable to the electron energy, the emission process should include the radiation reaction and quantum emission effects (*52*). In our simulations, these effects are self-consistently implemented in the particle-in-cell (PIC) code EPOCH (*53*, *54*) using a Monte Carlo method (*55*), which allows the self-consistent simulation of laser-plasma interactions in the strong electromagnetic radiation regime. The effects can be characterized by the radiation parameter

$$\chi_e = (e\hbar\epsilon_e/m_e^3c^5)|\mathbf{E}_\perp + \boldsymbol{\beta}\times\mathbf{B}| \quad (1)$$

Here, ϵ_e is the electron energy, $\mathbf{E}_\perp$ is the electric field perpendicular to the electron velocity $\boldsymbol{\beta} = \mathbf{v}/c$, and $F_\perp = |\mathbf{E}_\perp + \boldsymbol{\beta}\times\mathbf{B}| \approx \sqrt{(E_{sy} - B_{sz})^2 + (E_{sz} + B_{sy})^2}$ is the transverse electromagnetic field that arises from the self-generated electromagnetic fields in the plasma wake. Because the trapped electrons reside at the rear of the wake and the laser pulse locates at the very front of the wake, the laser fields do not interact directly with the trapped electrons and thus do not produce the radiation by laser-electron interaction. The radiation reaction effect on electron dynamics can be expressed as $\mathbf{f}_{rr} = -\frac{2}{3}\frac{m_e^2c^3}{\hbar}\alpha_f\chi_e^2\boldsymbol{\beta} \approx -6.4\times10^{15}\chi_e^2\boldsymbol{\beta}$[eV/m], where $\alpha_f = \frac{e^2}{\hbar c}$ is the fine-structure constant. Assuming $\chi_e^2 = 0.001$, the radiation reaction force ($|\mathbf{f}_{rr}| \approx 6.4$ TeV/m) becomes comparable with the electromagnetic force so that a substantial energy is transferred to high-energy photons. This strong emission has a notable impact on the electron dynamics, which should be treated using a stochastic quantum-loss model rather than using a classical continuous-loss model. Therefore, one needs to investigate the radiation process in laser-plasma interactions using self-consistent numerical simulations that include the quantum-corrected emission (*54*, *55*). The radiation power associated with radiation reaction and quantum effects can be expressed as $P_\gamma = \left(\frac{2m_e^2c^4\alpha_f}{3\hbar}\right)\chi_e^2 g(\chi_e)$, where $g(\chi_e) = \frac{3\sqrt{3}}{2\pi\chi_e^2}\int_0^{\frac{\chi_e}{2}} F(\chi_e,\chi_\gamma)d\chi_\gamma \approx 1/(1+4.8(1+\chi_e)\ln(1+1.7\chi_e)+2.44\chi_e^2)^{2/3}$ is the correction function due to quantum effects (*55*). As $g(\chi_e) \gtrsim 0.7$ for most of the emitting electrons with $\chi_e \lesssim 0.1$, one can approximately obtain

$$P_\gamma \approx \left(\frac{2\alpha_f\hbar e^2}{3m_e^4c^6}\right)\epsilon_e^2F_\perp^2 \quad (2)$$

Here, the characteristic radiated energy can be estimated as $\epsilon_\gamma \approx \left(\frac{4}{5\sqrt{3}}\frac{e\hbar}{m_e^3c^5}\right)\epsilon_e^2F_\perp$. By assuming that the initial electron energy

ϵ_e~5 GeV (before emitting γ-ray photons) and that the maximum transverse field $F_\perp \sim 3 \times 10^{13}$ V/m, the maximum photon energy of the γ-rays can reach GeV level.

Numerical simulations

Fully relativistic three-dimensional (3D) PIC simulations have been carried out by using the code EPOCH. A simulation window moving at the speed of light is used, which has absorbing boundary conditions for both fields and particles. The size of the window is 60 μm (x) × 45 μm (y) × 45 μm (z) with 1500 × 270 × 270 grid cells, sampled by four macroparticles in each cell. A plasma channel with a density profile of $n_e = n_0 + \Delta n_0$ is adopted to guide the high-power high-intensity laser pulse. Here, $\Delta n_0 = 0.3 a_0 n_c (r^2 \lambda_0^2 / \pi^2 r_0^4)$ is the channel depth, r is the radial distance from the channel axis, and the on-axis background density is set to $n_0 = 2 \times 10^{-4} a_0 n_c$ and $10^{-3} a_0 n_c$ in the acceleration and radiation stages, respectively, as shown in Fig. 2A. This type of plasma channels can be produced in several ways, such as using picosecond pulse laser–induced channeling (*15*, *56*, *57*) and laser-irradiated clusters (*58*). The incident linearly polarized laser pulse has a transversely Gaussian profile of $\exp(-r^2/r_0^2)$, a longitudinal distribution of $\sin^2(\pi t/2\tau_0)$, and a peak intensity of $I_0 = \frac{\pi}{2} \frac{m_e^2 c^5}{e^2 \lambda_0^2} a_0^2 \approx 4.9 \times 10^{21}$ W/cm^2 (amplitude $a_0 = 60$), where $r_0 = 10\lambda_0 = 10$ μm is the laser spot size and $\tau_0 = 30$ fs is the pulse duration (FWHM). The corresponding peak power is 7.7 PW for 232-J pulse energy. Such laser pulses are readily accessible from current multi-PW laser systems (*59*, *60*) and forthcoming laser facilities (*32*).

As a reference, we have carried out a larger-scale simulation case with the transverse dimensions of 90 μm (y) × 90 μm (z). The results are reported in the Supplementary Materials and are nearly the same as those discussed above. Furthermore, 3D PIC simulations indicate that, when the length of the plasma density up-ramp at the entrance of the radiator stage is within the range of 50 to 500 μm, it gives comparable results for the γ-ray emission. We have also carried out an additional simulation with reduced time step and cell size to investigate the effect of the numerical Cerenkov instability on the γ-ray generation, which indicates that there is no significant influence on the final results of this γ-ray radiation. The role of radiation reaction in our scheme is examined by the comparison of photon emission by energetic electrons with and without radiation reaction force, as described in the Supplementary Materials. This reveals that a self-consistently quantum-corrected radiation model must be taken into account in the emission of high-energy radiation by the electrons in extremely intense fields that we consider in this work.

SUPPLEMENTARY MATERIALS

Supplementary material for this article is available at http://advances.sciencemag.org/cgi/content/full/6/22/eaaz7240/DC1

REFERENCES AND NOTES

1. S. Corde, K. Ta Phuoc, G. Lambert, R. Fitour, V. Malka, A. Rousse, A. Beck, E. Lefebvre, Femtosecond X rays from laser-plasma accelerators. *Rev. Mod. Phys.* **85**, 1–48 (2013).
2. D. H. Bilderback, P. Elleaume, E. Weckert, Review of third and next generation synchrotron light sources. *J. Phys. B At. Mol. Opt. Phys.* **38**, S773–S797 (2005).
3. F. Albert, A. G. R. Thomas, Applications of laser wakefield accelerator-based light sources. *Plasma Phys. Control. Fusion* **58**, 103001 (2016).
4. B. Badelek, C. Blöchinger, J. Blümlein, E. Boos, R. Brinkmann, H. Burkhardt, P. Bussey, C. Carimalo, J. Chyla, A. K. Çiftçi, W. Decking, A. De Roeck, V. Fadin, M. Ferrario, A. Finch, H. Fraas, F. Franke, M. Galynskii, A. Gamp, I. Ginzburg, R. Godbole, D. S. Gorbunov, G. Gounaris, K. Hagiwara, L. Han, R.-D. Heuer, C. Heusch, J. Illana, V. Ilyin, P. Jankowski, Y. Jiang, G. Jikia, L. Jönsson, M. Kalachnikow, F. Kapusta, R. Klanner, M. Klassen, K. Kobayashi, T. Kon, G. Kotkin, M. Krämer, M. Krawczyk, Y. P. Kuang, E. Kuraev, J. Kwiecinski, M. Leenen, M. Levchuk, W. F. Ma, H. Martyn, T. Mayer, M. Melles, D. J. Miller, S. Mtingwa, M. Mühlleitner, B. Muryn, P. V. Nickles, R. Orava, G. Pancheri, A. Penin, A. Potylitsyn, P. Poulose, T. Quast, P. Raimondi, H. Redlin, F. Richard, S. D. Rindani, T. Rizzo, E. Saldin, W. Sandner, H. Schönnagel, E. Schneidmiller, H. J. Schreiber, S. Schreiber, K. P. Schüler, V. Serbo, A. Seryi, R. Shanidze, W. Da Silva, S. Söldner-rembold, M. Spira, A. M. Stasto, S. Sultansoy, T. Takahashi, V. Telnov, A. Tkabladze, D. Trines, A. Undrus, A. Wagner, N. Walker, I. Watanabe, T. Wengler, I. Will, S. Wipf, Ö. Yavaş, K. Yokoya, M. Yurkov, A. F. Zarnecki, P. Zerwas, F. Zomer, The photon collider at TESLA. *Int. J. Mod. Phys. A* **19**, 5097–5186 (2004).
5. M. Gari, H. Hebach, Photonuclear reactions at intermediate energies (40 MeV⩽Eγ⩽400 MeV). *Phys. Rep.* **72**, 1–55 (1981).
6. C. M. Tarbert, D. P. Watts, D. I. Glazier, P. Aguar, J. Ahrens, J. R. M. Annand, H. J. Arends, R. Beck, V. Bekrenev, B. Boillat, A. Braghieri, D. Branford, W. J. Briscoe, J. Brudvik, S. Cherepnya, R. Codling, E. J. Downie, K. Foehl, P. Grabmayr, R. Gregor, E. Heid, D. Hornidge, O. Jahn, V. L. Kashevarov, A. Knezevic, R. Kondratiev, M. Korolija, M. Kotulla, D. Krambrich, B. Krusche, M. Lang, V. Lisin, K. Livingston, S. Lugert, I. J. D. MacGregor, D. M. Manley, M. Martinez, J. C. McGeorge, D. Mekterovic, V. Metag, B. M. K. Nefkens, A. Nikolaev, R. Novotny, R. O. Owens, P. Pedroni, A. Polonski, S. N. Prakhov, J. W. Price, G. Rosner, M. Rost, T. Rostomyan, S. Schadmand, S. Schumann, D. Sober, A. Starostin, I. Supek, A. Thomas, M. Unverzagt, Th. Walcher, F. Zehr, Neutron skin of ^{208}Pb from coherent pion photoproduction. *Phys. Rev. Lett.* **112**, 242502 (2014).
7. ATLAS Collaboration, Evidence for light-by-light scattering in heavy-ion collisions with the ATLAS detector at the LHC. *Nat. Phys.* **13**, 852–858 (2017).
8. Y. Glinec, J. Faure, L. Le Dain, S. Darbon, T. Hosokai, J. J. Santos, E. Lefebvre, J. P. Rousseau, F. Burgy, B. Mercier, V. Malka, High-resolution γ-ray radiography produced by a laser-plasma driven electron source. *Phys. Rev. Lett.* **94**, 025003 (2005).
9. A. Sakdinawat, D. Attwood, Nanoscale X-ray imaging. *Nat. Photon.* **4**, 840–848 (2010).
10. W. Ackermann, G. Asova, V. Ayvazyan, A. Azima, N. Baboi, J. Bähr, V. Balandin, B. Beutner, A. Brandt, A. Bolzmann, R. Brinkmann, O. I. Brovko, M. Castellano, P. Castro, L. Catani, E. Chiadroni, S. Choroba, A. Cianchi, J. T. Costello, D. Cubaynes, J. Dardis, W. Decking, H. Delsim-Hashemi, A. Delserieys, G. Di Pirro, M. Dohlus, S. Düsterer, A. Eckhardt, H. T. Edwards, B. Faatz, J. Feldhaus, K. Flöttmann, J. Frisch, L. Fröhlich, T. Garvey, U. Gensch, Ch. Gerth, M. Görler, N. Golubeva, H.-J. Grabosch, M. Grecki, O. Grimm, K. Hacker, U. Hahn, J. H. Han, K. Honkavaara, T. Hott, M. Hüning, Y. Ivanisenko, E. Jaeschke, W. Jalmuzna, T. Jezynski, R. Kammering, V. Katalev, K. Kavanagh, E. T. Kennedy, S. Khodyachykh, K. Klose, V. Kocharyan, M. Körfer, M. Kollewe, W. Koprek, S. Korepanov, D. Kostin, M. Krassilnikov, G. Kube, M. Kuhlmann, C. L. S. Lewis, L. Lilje, T. Limberg, D. Lipka, F. Löhl, H. Luna, M. Luong, M. Martins, M. Meyer, P. Michelato, V. Miltchev, W. D. Möller, L. Monaco, W. F. O. Müller, O. Napieralski, O. Napoly, P. Nicolosi, D. Nölle, T. Nuñez, A. Oppelt, C. Pagani, R. Paparella, N. Pchalek, J. Pedregosa-Gutierrez, B. Petersen, B. Petrosyan, G. Petrosyan, L. Petrosyan, J. Pflüger, E. Plönjes, L. Poletto, K. Pozniak, E. Prat, D. Proch, P. Pucyk, P. Radcliffe, H. Redlin, K. Rehlich, M. Richter, M. Roehrs, J. Roensch, R. Romaniuk, M. Ross, J. Rossbach, V. Rybnikov, M. Sachwitz, E. L. Saldin, W. Sandner, H. Schlarb, B. Schmidt, M. Schmitz, P. Schmüser, J. R. Schneider, E. A. Schneidmiller, S. Schnepp, S. Schreiber, M. Seidel, D. Sertore, A. V. Shabunov, C. Simon, S. Simrock, E. Sombrowski, A. A. Sorokin, P. Spanknebel, R. Spesyvtsev, L. Staykov, B. Steffen, F. Stephan, F. Stulle, H. Thom, K. Tiedtke, M. Tischer, S. Toleikis, R. Treusch, D. Trines, I. Tsakov, E. Vogel, T. Weiland, H. Weise, M. Wellhöfer, M. Wendt, I. Will, A. Winter, K. Wittenburg, W. Wurth, P. Yeates, M. V. Yurkov, I. Zagorodnov, K. Zapfe, Operation of a free-electron laser from the extreme ultraviolet to the water window. *Nat. Photon.* **1**, 336–342 (2007).
11. T. Tajima, J. Dawson, Laser electron accelerator. *Phys. Rev. Lett.* **43**, 267–270 (1979).
12. A. Pukhov, J. Meyer-ter-Vehn, Laser wake field acceleration: The highly non-linear broken-wave regime. *Appl. Phys. B* **74**, 355–361 (2002).
13. K. Nakajima, D. Fisher, T. Kawakubo, H. Nakanishi, A. Ogata, Y. Kato, Y. Kitagawa, R. Kodama, K. Mima, H. Shiraga, K. Suzuki, K. Yamakawa, T. Zhang, Y. Sakawa, T. Shoji, Y. Nishida, N. Yugami, M. Downer, T. Tajima, Observation of ultrahigh gradient electron acceleration by a self-modulated intense short laser pulse. *Phys. Rev. Lett.* **74**, 4428–4431 (1995).
14. S. P. D. Mangles, C. D. Murphy, Z. Najmudin, A. G. R. Thomas, J. L. Collier, A. E. Dangor, E. J. Divall, P. S. Foster, J. G. Gallacher, C. J. Hooker, D. A. Jaroszynski, A. J. Langley, W. B. Mori, P. A. Norreys, F. S. Tsung, R. Viskup, B. R. Walton, K. Krushelnick, Monoenergetic beams of relativistic electrons from intense laser–plasma interactions. *Nature* **431**, 535–538 (2004).
15. C. G. R. Geddes, Cs. Toth, J. van Tilborg, E. Esarey, C. B. Schroeder, D. Bruhwiler, C. Nieter, J. Cary, W. P. Leemans, High-quality electron beams from a laser wakefield accelerator using plasma-channel guiding. *Nature* **431**, 538–541 (2004).

16. J. Faure, Y. Glinec, A. Pukhov, S. Kiselev, S. Gordienko, E. Lefebvre, J.-P. Rousseau, F. Burgy, V. Malka, A laser–plasma accelerator producing monoenergetic electron beams. *Nature* **431**, 541–544 (2004).
17. E. Esarey, C. B. Schroeder, W. P. Leemans, Physics of laser-driven plasma-based electron accelerators. *Rev. Mod. Phys.* **81**, 1229–1285 (2009).
18. A. J. Gonsalves, K. Nakamura, J. Daniels, C. Benedetti, C. Pieronek, T. C. H. de Raadt, S. Steinke, J. H. Bin, S. S. Bulanov, J. van Tilborg, C. G. R. Geddes, C. B. Schroeder, Cs. Tóth, E. Esarey, K. Swanson, L. Fan-Chiang, G. Bagdasarov, N. Bobrova, V. Gasilov, G. Korn, P. Sasorov, W. P. Leemans, Petawatt laser guiding and electron beam acceleration to 8 GeV in a laser-heated capillary discharge waveguide. *Phys. Rev. Lett.* **122**, 084801 (2019).
19. H. P. Schlenvoigt, K. Haupt, A. Debus, F. Budde, O. Jäckel, S. Pfotenhauer, H. Schwoerer, E. Rohwer, J. G. Gallacher, E. Brunetti, R. P. Shanks, S. M. Wiggins, D. A. Jaroszynski, A compact synchrotron radiation source driven by a laser-plasma wakefield accelerator. *Nat. Phys.* **4**, 130–133 (2008).
20. S. Kneip, C. McGuffey, J. L. Martins, S. F. Martins, C. Bellei, V. Chvykov, F. Dollar, R. Fonseca, C. Huntington, G. Kalintchenko, A. Maksimchuk, S. P. D. Mangles, T. Matsuoka, S. R. Nagel, C. A. J. Palmer, J. Schreiber, K. Ta Phuoc, A. G. R. Thomas, V. Yanovsky, L. O. Silva, K. Krushelnick, Z. Najmudin, Bright spatially coherent synchrotron X-rays from a table-top source. *Nat. Phys.* **6**, 980–983 (2010).
21. S. Cipiccia, M. R. Islam, B. Ersfeld, R. P. Shanks, E. Brunetti, G. Vieux, X. Yang, R. C. Issac, S. M. Wiggins, G. H. Welsh, M.-P. Anania, D. Maneuski, R. Montgomery, G. Smith, M. Hoek, D. J. Hamilton, N. R. C. Lemos, D. Symes, P. P. Rajeev, V. O. Shea, J. M. Dias, D. A. Jaroszynski, Gamma-rays from harmonically resonant betatron oscillations in a plasma wake. *Nat. Phys.* **7**, 867–871 (2011).
22. J. Wenz, S. Schleede, K. Khrennikov, M. Bech, P. Thibault, M. Heigoldt, F. Pfeiffer, S. Karsch, Quantitative X-ray phase-contrast microtomography from a compact laser-driven betatron source. *Nat. Commun.* **6**, 7568 (2015).
23. K. Ta Phuoc, S. Corde, C. Thaury, V. Malka, A. Tafzi, J. P. Goddet, R. C. Shah, S. Sebban, A. Rousse, All-optical Compton gamma-ray source. *Nat. Photon.* **6**, 308–311 (2012).
24. S. Chen, N. D. Powers, I. Ghebregziabher, C. M. Maharjan, C. Liu, G. Golovin, S. Banerjee, J. Zhang, N. Cunningham, A. Moorti, S. Clarke, S. Pozzi, D. P. Umstadter, MeV-energy X rays from inverse Compton scattering with laser-wakefield accelerated electrons. *Phys. Rev. Lett.* **110**, 155003 (2013).
25. G. Sarri, D. J. Corvan, W. Schumaker, J. M. Cole, A. Di Piazza, H. Ahmed, C. Harvey, C. H. Keitel, K. Krushelnick, S. P. D. Mangles, Z. Najmudin, D. Symes, A. G. R. Thomas, M. Yeung, Z. Zhao, M. Zepf, Ultrahigh brilliance multi-MeV γ-ray beams from nonlinear relativistic thomson scattering. *Phys. Rev. Lett.* **113**, 224801 (2014).
26. J. A. Holloway, P. A. Norreys, A. G. R. Thomas, R. Bartolini, R. Bingham, J. Nydell, R. M. G. M. Trines, R. Walker, M. Wing, Brilliant X-rays using a two-stage plasma insertion device. *Sci. Rep.* **7**, 3985 (2017).
27. J. Ferri, S. Corde, A. Döpp, A. Lifschitz, A. Doche, C. Thaury, K. Ta. Phuoc, B. Mahieu, I. A. Andriyash, V. Malka, X. Davoine, High-brilliance betatron γ-ray source powered by laser-accelerated electrons. *Phys. Rev. Lett.* **120**, 254802 (2018).
28. K. Ta Phuoc, E. Esarey, V. Leurent, E. Cormier-Michel, C. G. R. Geddes, C. B. Schroeder, A. Rousse, W. P. Leemans, Betatron radiation from density tailored plasmas. *Phys. Plasmas* **15**, 063102 (2008).
29. G. A. Mourou, T. Tajima, S. V. Bulanov, Optics in the relativistic regime. *Rev. Mod. Phys.* **78**, 309–371 (2006).
30. M. Marklund, P. K. Shukla, Nonlinear collective effects in photon-photon and photon-plasma interactions. *Rev. Mod. Phys.* **78**, 591–640 (2006).
31. A. Di Piazza, C. Müller, K. Z. Hatsagortsyan, C. H. Keitel, Extremely high-intensity laser interactions with fundamental quantum systems. *Rev. Mod. Phys.* **84**, 1177–1228 (2012).
32. The next generation 10 PW-level laser facilities, such as Extreme Light Infrastructure - Nuclear Physics (ELI-NP, http://www.eli-np.ro), Exawatt Center for Extreme Light Studies (XCELS, https://xcels.iapras.ru), Apollon Laser (https://apollonlaserfacility.cnrs.fr/en/home/), and Vulcan Laser (https://www.clf.stfc.ac.uk/Pages/Vulcan-2020.aspx).
33. X.-L. Zhu, T.-P. Yu, Z.-M. Sheng, Y. Yin, I. C. E. Turcu, A. Pukhov, Dense GeV electron-positron pairs generated by lasers in near-critical-density plasmas. *Nat. Commun.* **7**, 13686 (2016).
34. X.-L. Zhu, Y. Yin, T.-P. Yu, F.-Q. Shao, Z.-Y. Ge, W.-Q. Wang, J.-J. Liu, Enhanced electron trapping and γ ray emission by ultra-intense laser irradiating a near-critical-density plasma filled gold cone. *New J. Phys.* **17**, 053039 (2015).
35. T. W. Huang, C. M. Kim, C. T. Zhou, M. H. Cho, K. Nakajima, C. M. Ryu, S. C. Ruan, C. H. Nam, Highly efficient laser-driven Compton gamma-ray source. *New J. Phys.* **21**, 013008 (2019).
36. T. Nakamura, J. K. Koga, T. Z. Esirkepov, M. Kando, G. Korn, S. V. Bulanov, High-power γ-ray flash generation in ultraintense laser-plasma interactions. *Phys. Rev. Lett.* **108**, 195001 (2012).
37. L. L. Ji, A. Pukhov, I. Y. Kostyukov, B. F. Shen, K. Akli, Radiation-reaction trapping of electrons in extreme laser fields. *Phys. Rev. Lett.* **112**, 145003 (2014).
38. X.-L. Zhu, T.-P. Yu, M. Chen, S.-M. Weng, Z.-M. Sheng, Generation of GeV positron and γ-photon beams with controllable angular momentum by intense lasers. *New J. Phys.* **20**, 083013 (2018).
39. D. J. Stark, T. Toncian, A. V. Arefiev, Enhanced multi-MeV photon emission by a laser-driven electron beam in a self-generated magnetic field. *Phys. Rev. Lett.* **116**, 185003 (2016).
40. W.-M. Wang, Z.-M. Sheng, P. Gibbon, L.-M. Chen, Y.-T. Li, J. Zhang, Collimated ultrabright gamma rays from electron wiggling along a petawatt laser-irradiated wire in the QED regime. *Proc. Natl. Acad. Sci. U.S.A.* **115**, 9911–9916 (2018).
41. T. W. Huang, C. M. Kim, C. T. Zhou, C. M. Ryu, K. Nakajima, S. C. Ruan, C. H. Nam, Tabletop laser-driven gamma-ray source with nanostructured double-layer target. *Plasma Phys. Control. Fusion* **60**, 115006 (2018).
42. T. G. Blackburn, C. P. Ridgers, J. G. Kirk, A. R. Bell, Quantum radiation reaction in laser-electron-beam collisions. *Phys. Rev. Lett.* **112**, 015001 (2014).
43. M. Lobet, X. Davoine, E. d'Humières, L. Gremillet, Generation of high-energy electron-positron pairs in the collision of a laser-accelerated electron beam with a multipetawatt laser. *Phys. Rev. Accel. Beams* **20**, 043401 (2017).
44. S. S. Bulanov, C. B. Schroeder, E. Esarey, W. P. Leemans, Electromagnetic cascade in high-energy electron, positron, and photon interactions with intense laser pulses. *Phys. Rev. A* **87**, 062110 (2013).
45. A. Gonoskov, A. Bashinov, S. Bastrakov, E. Efimenko, A. Ilderton, A. Kim, M. Marklund, I. Meyerov, A. Muraviev, A. Sergeev, Ultrabright GeV photon source via controlled electromagnetic cascades in laser-dipole waves. *Phys. Rev. X* **7**, 041003 (2017).
46. A. Benedetti, M. Tamburini, C. H. Keitel, Giant collimated gamma-ray flashes. *Nat. Photon.* **12**, 319–323 (2018).
47. S. Gordienko, A. Pukhov, Scalings for ultrarelativistic laser plasmas and quasimonoenergetic electrons. *Phys. Plasmas* **12**, 043109 (2005).
48. J. M. Cole, K. T. Behm, E. Gerstmayr, T. G. Blackburn, J. C. Wood, C. D. Baird, M. J. Duff, C. Harvey, A. Ilderton, A. S. Joglekar, K. Krushelnick, S. Kuschel, M. Marklund, P. McKenna, C. D. Murphy, K. Poder, C. P. Ridgers, G. M. Samarin, G. Sarri, D. R. Symes, A. G. R. Thomas, J. Warwick, M. Zepf, Z. Najmudin, S. P. D. Mangles, Experimental evidence of radiation reaction in the collision of a high-intensity laser pulse with a laser-wakefield accelerated electron beam. *Phys. Rev. X* **8**, 011020 (2018).
49. K. Poder, M. Tamburini, G. Sarri, A. Di Piazza, S. Kuschel, C. D. Baird, K. Behm, S. Bohlen, J. M. Cole, D. J. Corvan, M. Duff, E. Gerstmayr, C. H. Keitel, K. Krushelnick, S. P. D. Mangles, P. McKenna, C. D. Murphy, Z. Najmudin, C. P. Ridgers, G. M. Samarin, D. R. Symes, A. G. R. Thomas, J. Warwick, M. Zepf, Experimental signatures of the quantum nature of radiation reaction in the field of an ultraintense laser. *Phys. Rev. X* **8**, 031004 (2018).
50. O. J. Pike, F. Mackenroth, E. G. Hill, S. J. Rose, A photon-photon collider in a vacuum hohlraum. *Nat. Photon.* **8**, 434–436 (2014).
51. J. Q. Yu, H. Y. Lu, T. Takahashi, R. H. Hu, Z. Gong, W. J. Ma, Y. S. Huang, C. E. Chen, X. Q. Yan, Creation of electron-positron pairs in photon-photon collisions driven by 10-PW laser pulses. *Phys. Rev. Lett.* **122**, 014802 (2019).
52. V. I. Ritus, Quantum effects of the interaction of elementary particles with an intense electromagnetic field. *J. Sov. Laser Res.* **6**, 497–617 (1985).
53. T. D. Arber, K. Bennett, C. S. Brady, A. Lawrence-Douglas, M. G. Ramsay, N. J. Sircombe, P. Gillies, R. G. Evans, H. Schmitz, A. R. Bell, C. P. Ridgers, Contemporary particle-in-cell approach to laser-plasma modelling. *Plasma Phys. Control. Fusion* **57**, 113001 (2015).
54. C. P. Ridgers, C. S. Brady, R. Duclous, J. G. Kirk, K. Bennett, T. D. Arber, A. P. L. Robinson, A. R. Bell, Dense electron-positron plasmas and ultraintense γ rays from laser-irradiated solids. *Phys. Rev. Lett.* **108**, 165006 (2012).
55. C. P. Ridgers, J. G. Kirk, R. Duclous, T. G. Blackburn, C. S. Brady, K. Bennett, T. D. Arber, A. R. Bell, Modelling gamma-ray photon emission and pair production in high-intensity laser–matter interactions. *J. Comput. Phys.* **260**, 273–285 (2014).
56. M. Borghesi, A. J. MacKinnon, L. Barringer, R. Gaillard, L. A. Gizzi, C. Meyer, O. Willi, A. Pukhov, J. Meyer-ter-Vehn, Relativistic channeling of a picosecond laser pulse in a near-critical preformed plasma. *Phys. Rev. Lett.* **78**, 879–882 (1997).
57. Y. Mizuta, T. Hosokai, S. Masuda, A. Zhidkov, K. Makito, N. Nakanii, S. Kajino, A. Nishida, M. Kando, M. Mori, H. Kotaki, Y. Hayashi, S. V. Bulanov, R. Kodama, Splash plasma channels produced by picosecond laser pulses in argon gas for laser wakefield acceleration. *Phys. Rev. ST Accel. Beams* **15**, 121301 (2012).
58. Y. Fukuda, A. Ya. Faenov, M. Tampo, T. A. Pikuz, T. Nakamura, M. Kando, Y. Hayashi, A. Yogo, H. Sakaki, T. Kameshima, A. S. Pirozhkov, K. Ogura, M. Mori, T. Zh. Esirkepov, J. Koga, A. S. Boldarev, V. A. Gasilov, A. I. Magunov, T. Yamauchi, R. Kodama, P. R. Bolton, Y. Kato, T. Tajima, H. Daido, S. V. Bulanov, Energy increase in multi-MeV ion acceleration in the interaction of a short pulse laser with a cluster-gas target. *Phys. Rev. Lett.* **103**, 165002 (2009).
59. J. H. Sung, H. W. Lee, J. Y. Yoo, J. W. Yoon, C. W. Lee, J. M. Yang, Y. J. Son, Y. H. Jang, S. K. Lee, C. H. Nam, 4.2 PW, 20 fs Ti:sapphire laser at 0.1 Hz. *Opt. Lett.* **42**, 2058–2061 (2017).
60. W. Li, Z. Gan, L. Yu, C. Wang, Y. Liu, Z. Guo, L. Xu, M. Xu, Y. Hang, Y. Xu, J. Wang, P. Huang, H. Cao, B. Yao, X. Zhang, L. Chen, Y. Tang, S. Li, X. Liu, S. Li, M. He, D. Yin, X. Liang, Y. Leng, R. Li, Z. Xu, 339 J high-energy Ti:sapphire chirped-pulse amplifier for 10 PW laser facility. *Opt. Lett.* **43**, 5681–5684 (2018).

Acknowledgments
Funding: The work was supported by the National Key Research and Development Program of China (grant no. 2018YFA0404802), the National Natural Science Foundation of China (grant nos. 11721091, 11991074, 11775144, 11774227, 11622547, and 11775302), the Strategic Priority Research Program of Chinese Academy of Sciences (grant nos. XDA25050100 and XDA25050300) and Science Challenge Project (grant no. TZ2018005). X.-L.Z. acknowledges support from the China Scholarship Council. This work has received funding from the European Union's Horizon 2020 research and innovation programme under the Marie Skłodowska-Curie (grant no. 743949), project EuPRAXIA (grant no. 653782), LASERLAB-EUROPE (grant no. 654148), EuCARD-2 (grant no. 312453), ARIES (grant no. 730871), UK Engineering and Physical Sciences Research Council (EPSRC; grant no. EP/N028694/1), and the Extreme Light Infrastructure (ELI) European Projects. The development of EPOCH was partly funded by the EPSRC (grant no. EP/G056803/1). Simulations were performed on the PI supercomputer at Shanghai Jiao Tong University, the ARCHER supercomputer in Edinburgh, and the Tianhe-2 supercomputer at the National Supercomputer Center in Guangzhou. Access to ARCHER is via Plasma HEC Consortium supported by EPSRC (nos. EP/L000237/1 and EP/R029148/1). **Author contributions:** X.-L.Z., Z.-M.S., and M.C. conceived the scheme. X.-L.Z. performed the simulations. X.-L.Z., Z.-M.S., and M.C. developed the analytical model and wrote the manuscript with input from all coauthors. S.-M.W., T.-P.Y., W.-M.W., F.H., P.M., D.A.J., and J.Z. interpreted details of the results. Z.-M.S., M.C., and J.Z. supervised the study. All authors discussed the results and reviewed the manuscript. **Competing interests:** The authors declare that they have no competing interests. **Data and materials availability:** All data needed to evaluate the conclusions in the paper are present in the paper and/or the Supplementary Materials. Additional data related to this paper may be requested from the authors. Input scripts for the simulations underpinning this work are openly available from the University of Strathclyde Knowledge Base at https://doi.org/10.15129/2e322ff9-e631-4a08-ba4e-838dd30a5f1d.

Submitted 9 October 2019
Accepted 1 April 2020
Published 29 May 2020
10.1126/sciadv.aaz7240

Citation: X.-L. Zhu, M. Chen, S.-M. Weng, T.-P. Yu, W.-M. Wang, F. He, Z.-M. Sheng, P. McKenna, D. A. Jaroszynski, J. Zhang, Extremely brilliant GeV γ-rays from a two-stage laser-plasma accelerator. *Sci. Adv.* **6**, eaaz7240 (2020).